

# DeepForgeSeal: Latent Space-Driven Semi-Fragile Watermarking for Deepfake Detection Using Multi-Agent Adversarial Reinforcement Learning

Tharindu Fernando, *Member, IEEE*, Clinton Fookes, *Senior Member, IEEE*, and Sridha Sridharan, *Life Senior Member, IEEE*.

**Abstract**—Rapid advances in generative AI have led to increasingly realistic deepfakes, posing growing challenges for law enforcement and public trust. Existing passive deepfake detectors struggle to keep pace, largely due to their dependence on specific forgery artifacts, which limits their ability to generalize to new deepfake types. Proactive deepfake detection using watermarks has emerged to address the challenge of identifying high-quality synthetic media. However, these methods often struggle to balance robustness against benign distortions with sensitivity to malicious tampering. This paper introduces a novel deep learning framework that harnesses high-dimensional latent space representations and the Multi-Agent Adversarial Reinforcement Learning (MAARL) paradigm to develop a robust and adaptive watermarking approach. Specifically, we develop a learnable watermark embedder that operates in the latent space, capturing high-level image semantics, while offering precise control over message encoding and extraction. The MAARL paradigm empowers the learnable watermarking agent to pursue an optimal balance between robustness and fragility by interacting with a dynamic curriculum of benign and malicious image manipulations simulated by an adversarial attacker agent. Comprehensive evaluations on the CelebA and CelebA-HQ benchmarks reveal that our method consistently outperforms state-of-the-art approaches, achieving improvements of over 4.5% on CelebA and more than 5.3% on CelebA-HQ under challenging manipulation scenarios.

**Index Terms**—Deepfake Detection, Semi-Fragile Watermarks, Multi-Agent Adversarial Reinforcement Learning, Digital Forensics

## I. INTRODUCTION

Generative AI has rapidly transformed the way we create and edit multimedia, making it faster and easier than ever to produce high-quality images, audio, and video. While these innovations unlock exciting possibilities, they also introduce serious risks. Among the most concerning threats are image and video deepfakes, highly realistic, AI-generated images and videos that mimic real persons, posing significant challenges, not only for their role in spreading misinformation and disinformation at an alarming pace but also for their implications on privacy, consent, security, and societal trust [1], [2], [3], [4], [5].

To combat the rapid spread of deepfakes, watermarking has emerged as a technique that allows users to validate the authenticity and integrity of the multimedia they consume. A robust watermarking technique should be resilient to

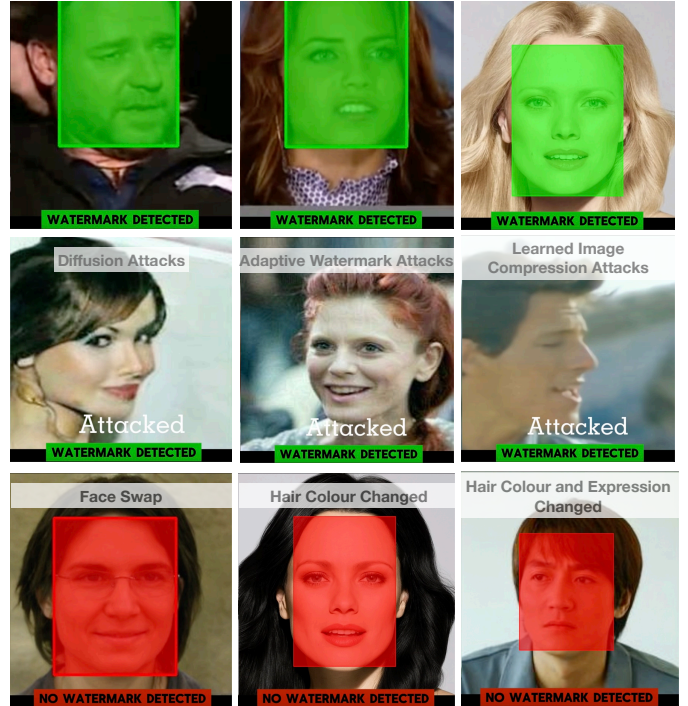


Fig. 1. Watermarking and watermark retrieval performance of proposed *DeepForgeSeal* framework. The visualisations include low-resolution and high-resolution bonafide images (row 1), numerous learned attacks against watermarking (row 2), and watermarked images that have undergone semantic-altering manipulations (row 3).

distortions such as JPEG compression, cropping, and colour changes to keep the embedded watermark intact. While being resilient to such incidental distortions, a good watermarking technique should demonstrate fragility towards content-altering modifications, such as face-swapping-type malicious edits that alter the semantic-level meaning of the image. Recently, deep learning techniques [6], [7], [8], [9], [10] have made significant progress towards achieving this paradoxical combination of resilience and fragility. For instance, SepMark [8] introduced an encoder–decoder architecture featuring a unified encoder for watermark embedding and two distinct decoders designed to recover the watermark under varying robustness constraints, thereby enabling selective resilience against different levels of adversarial distortion. However, most existing deep watermarking techniques for deepfake detection rely on a fixed, pre-defined watermark location for extraction,

T. Fernando, C. Fookes, and S. Sridharan are with The Signal Processing, Artificial Intelligence and Vision Technologies (SAIVT), Queensland University of Technology, Australia.

which makes them vulnerable, as perpetrators can easily detect and tamper the watermark once its position is known. In addition, these methods often lack robustness against benign image manipulations such as brightness adjustments or heavy compression, leading to a high rate of false positives in deepfake detection. Furthermore, current supervised and adversarial learning approaches provide only limited fidelity in addressing the resilience–fragility paradox.

Most recently, OmniGuard [9] introduced a more flexible approach for image manipulation detection and localisation by incorporating a degradation-aware tamper extraction network designed for blind, robust copyright protection and tamper localization. However, the framework embeds watermarks directly in the pixel space, which makes them more susceptible to attacks. Even minor changes in image orientation or scale can significantly alter pixel values, making pixel-based systems highly sensitive to trivial modifications despite the semantic content remaining unchanged. Consequently, the OmniGuard framework is less effective in detecting deepfakes, where the primary objective is to identify only malicious edits that alter the semantic-level meaning of the image.

In contrast to existing methods, we embed watermarks in the latent space rather than the pixel space, leveraging semantic-level manipulations of the image’s representation. Since the latent space encodes high-level meaning, the watermark becomes tightly coupled with the image’s semantics. Any malicious attempt to alter the image’s meaning disrupts this coupling, effectively breaking the watermark and revealing tampering. Most importantly, through a learnable watermark embedder network, we identify less perceptually salient directions to embed information without significantly altering the human-perceived semantics of the input image. We propose to leverage a spherical latent space for the embedding of the proposed watermark, which offers normalised operations for the embedding of our watermark, preventing the watermark embedder from drifting arbitrarily far from the original input representation, and making significant changes.

Embedding the watermark in this space offers two key advantages: (1) inherent resilience to benign transformations, such as resizing, compression, or brightness adjustments, that do not significantly alter semantic features, and (2) heightened sensitivity to malicious manipulations that change the semantic meaning of the image, such as identity swaps or expression alterations in deepfakes. By disentangling the watermark from the pixel domain and leveraging semantic representations, our approach aligns watermarking with the very nature of generative models, making it both resilient and semantically aware.

We propose a novel Multi-agent Adversarial Reinforcement Learning (MAARL) paradigm for learning watermarks that are both resilient to benign manipulations and fragile to semantic alterations, enabling robust deepfake detection. The framework is structured as a multi-objective game between two agents: the watermarking agent (i.e., the watermark embedder, extractor), and the attacker. The watermarking agents aim to embed latent space watermarks that survive traditional image transformations but fail under semantic changes. The attacker, in turn, seeks to break the watermark by maximizing extractor loss. It

can dynamically adjust the strength and type of attacks, ranging from conventional (e.g., compression, resizing) to semantic (e.g., facial attribute editing via StyleGAN), and combine them into complex, evolving curricula. This adversarial setup forces the watermarking agent to learn a sophisticated strategy that balances robustness and fragility, avoiding both overly weak and excessively strong watermarking schemes, allowing us to arrive at the right combination for this paradoxical objective. The result is an architecture that achieves unprecedented levels of resilience across bonafide transformations and greater levels of fragility towards malicious manipulations (See Fig. 1). The main technical contributions of this paper, through which we introduce the proposed *DeepForgeSeal* framework, can be summarised as follows:

- 1) We introduce a novel deep watermarking framework for deepfake detection that operates in the high-dimensional semantic space of input images.
- 2) We design a learnable watermarking agent with explicit control over message encoding and extraction, achieving semantic stealth.
- 3) We propose a new MAARL (Multi Agent Adversarial Reinforcement Learning) paradigm that enables the agent to learn a strategy balancing watermark resilience and fragility.
- 4) We develop a reward function that guides the watermark attacker to discover failure regions in the latent space and image manipulations that induce significant latent shifts, allowing it to devise a structured curriculum of attacks.

## II. RELATED WORK

### A. Watermarking Approaches for Deepfake Detection

Passive deepfake detection refers to techniques that analyse the media without requiring any prior knowledge of the generation process or embedding of security features such as watermarks. These approaches have demonstrated remarkable performance over the past decade, primarily by identifying artefacts introduced during the deepfake generation process, such as unsynchronised lip movements [11], irregular facial landmarks [12], or physiological inconsistencies like abnormal blood oxygen concentration [13]. However, their effectiveness is inherently tied to the presence of such artefacts, which vary depending on the generation technique used. Consequently, the generalisability of these detectors to novel or unseen deepfake generation methods remains limited. Moreover, the rapid evolution of deepfake technologies poses a significant challenge to maintaining detection robustness, raising concerns about the long-term reliability of passive detection strategies. Such limitations have led to the development of proactive deepfake detection approaches, with watermarking being a prominent example. This technique embeds invisible signals into benign images before any manipulation occurs. These signals act as verification markers, enabling systems to actively determine whether the content has been tampered with based on the presence and integrity of the embedded watermark.

One of the earliest works in watermarking based deepfake detection can be attributed to [14], which embeds a robust,

invisible watermark into facial images before any manipulation occurs. These watermarks are resilient to various deepfake transformations and image processing operations. The embedded watermark acts as a unique identifier, allowing the origin of a manipulated image to be traced. The works [15], [16] have also leveraged the concept of robust watermarking as a line of defense against deepfakes. Specifically, in contrast to [14], which embeds identity-linked tags using a learned network which is resilient to deepfake transformations, [15], [16] introduce training-free watermarking mechanisms based on facial landmarks. For example, instead of relying on learned embeddings, the authors of [16] propose to transform structural facial representations into binary perceptual watermarks, enabling robust and imperceptible embedding without extensive model training. Despite these advances, robust watermarking-based deepfake detection approaches require validating the embedded watermark against a known source or identity, which can be logistically complex in real-world applications, such as in social media platforms. Each image or video must be checked to ensure the watermark matches a trusted source identity, which assumes access to and maintenance of such a database.

Semi-fragile watermarks, which leverage both the fragility and robustness of watermarking, simplify the detection process by serving as self-contained integrity checks. Specifically, if the watermark is broken or unreadable, it directly signals tampering, without needing to compare against a source, making them more efficient and scalable for deployment in environments where rapid and autonomous verification is critical. One of the early works in semi-fragile watermarks for deepfake detection can be attributed to FaceGuard [17], which encodes a semi-fragile identity-specific watermark. Along similar lines, Zhao et al. [6] proposed an identity-based semi-fragile watermarking approach that is sensitive to face swap manipulations while remaining resilient to benign image transformations. Despite its advances, the reliance on identity-specific watermarks for each individual makes these techniques less appealing for real-world applications in which the true identity of the individuals is not available or cannot be readily extracted. WaterLo [18] addresses these limitations by introducing a localised, fixed semi-fragile watermark that disappears in manipulated regions, allowing not only detection but also precise localisation of tampered areas. Following this approach, the authors of FaceSigns [19] have introduced a semi-fragile watermarking framework that embeds a 128-bit secret message directly into the image pixels.

Most recently, the EditGuard [10] introduces a novel approach for decoupling the training process from specific tampering types. Traditional watermarking systems often require retraining or fine-tuning for each manipulation scenario. In contrast, EditGuard’s image-to-image steganography framework generalises across diverse tampering methods, including face swaps, background replacements, and AI-generated edits, without needing retraining. OmniGuard [9] further enhances this approach by introducing a hybrid forensic framework that combines proactive embedding of the semi-fragile watermark with passive blind extraction. In a different line of work, the authors of [7] leverage the mathematical properties of

fractals to generate watermark patterns through a parameter-driven pipeline. Moreover, watermarks are embedded using an entry-to-patch strategy, where each watermark matrix entry is mapped to a specific image patch, enabling precise localisation of manipulated regions. Though significant strides have been made, the majority of existing semi-fragile watermarking approaches still rely on the pixel space for embedding, rather than leveraging the latent space, which could offer greater flexibility and robustness. Furthermore, current adversarial training pipelines used when training the watermarking frameworks are often simplistic and lack the sophistication needed to simulate complex attack curricula. As a result, the resilience of watermarking techniques under realistic and increasingly sophisticated adversarial conditions remains limited. In contrast, by leveraging a spherical latent space, our framework ensures more structured and disentangled representations, which enhances watermark embedding consistency, robustness, and manipulation sensitivity. Additionally, the integration of MAARL enables the system to simulate and defend against complex, curriculum-based adversarial attacks, significantly improving the robustness and generalisability of the watermarking strategy across diverse manipulation scenarios.

## B. Multi Agent Adversarial Reinforcement Learning

In multi-agent learning setting the relationships among agents can be categorised into corporative, competitive, and both [20], while most of the prior works [21], [22], [23], [24], [25] in Multi Agent Reinforcement Learning (MARL) have focused on cooperative tasks, in which the cumulative reward is maximized as a group. Among the limited number of work extending traditional MARL into adversarial settings, researchers have introduced adversarial elements, either as competing agents or perturbations, to enhance the robustness and generalisation capabilities of the overall algorithm. For example, in [26] the authors have shown the potential of learning a robust generalise policy using Multi Agent Adversarial Reinforcement Learning (MAARL), where as in the authors of [27] have used MAARL to avoid overfitting. In a similar line of work, Bukharin et. al [28] address the lack robustness and sensitivity to environment changes in MARL through adversarial training. Specifically, the authors of [28] introduce adversarial regularization to enforce Lipschitz continuity in policies, improving robustness against noisy observations. Most recently, Yuan et. al [29] have proposed an approach based on evolutionary learning to enhance robustness in message-passing for improving the communication efficiency of agents.

While adversarial training has shown promise in both MARL and watermarking independently, to the best of our knowledge, none of the prior works have investigated the integration of MAARL into watermarking. Through empirical evaluations we demonstrate that MAARL offers a compelling framework to train watermarking agents that can dynamically adapt to image manipulations, potentially leading to watermarking systems that are both robust and semi-fragile, providing resistant to benign transformations yet sensitive to malicious tampering.

### III. METHODS

In this section, we discuss our proposed approach. We first provide an overview of the main components that constitute our DeepForgeSeal framework in Sec. III-A. Our watermarking agent, watermark attacker, and watermark extraction and deepfake detection processes are discussed in Secs. III-B, III-C, and III-D, respectively. Finally, implementation details of the framework are discussed in Sec. III-E.

#### A. Overview

Given an input image  $x$ , we define a watermarking agent  $\theta$  that learns the distribution of the semantic features  $f(x)$ , projects these features into a spherical latent space  $\mathbb{S}$ , inserts a watermark  $w_x$  in the latent space ensuring that it does not significantly alter the semantic meaning of  $x$ , and decodes the new image  $x_w$  with the watermark from the spherical latent space back to the image space. The objective of the watermarking agent is to identify the region in  $\mathbb{S}$  where it could embed the watermark without significantly altering the human-perceived meaning of  $x$ . Similarly, it should learn to maintain an optimal balance between the resilience of the embedded watermark towards benign operations, such as JPEG compression, cropping, and color adjustments, and its fragility to malicious edits, such as face swapping and facial attribute editing, that alter the semantic content of the image.

The objective of the watermark attacker agent,  $\eta$ , is to generate an adversarial image  $x_a$  from the watermarked image  $x_w$ , i.e.,  $\eta(x_w) \rightarrow x_a$ , by applying transformations that degrade or remove the embedded watermark. To achieve this, the attacker can choose from a range of image manipulations, including benign operations and malicious edits. These manipulations may also be combined, and for each type, the agent can control the associated parameters to vary the strength of the attack.

The watermark extractor,  $\delta$ , is responsible for retrieving the embedded watermark from a given image  $x'$ . Since the watermarking agent  $\theta$  dynamically adjusts both the location and content of the watermark, the extractor must co-adapt and learn in tandem with the watermarking agent to ensure reliable extraction. In our framework, the success or failure of watermark extraction serves as a heuristic for deepfake detection. Specifically, if the extractor  $\delta$  fails to recover a valid watermark from the image  $x'$ , the image is flagged as a potential deepfake. Our approach leverages the learned consistency between the watermarking and extraction processes as an indirect signal of authenticity, enabling the detection of semantic-level manipulations without relying on a fixed watermark pattern. These modules, and the flow of information between them, are illustrated in Fig. 2.

#### B. Watermarking Agent

The watermarking agent is responsible for encoding and embedding the watermark into the image. Its architecture is designed to operate within the semantic latent space of a pre-trained CLIP model, ensuring that the embedding process is guided by high-level image representations. The procedure comprises two key stages: (i) directional embedding in the

latent sphere, and (ii) perturbative watermark embedding. These stages are discussed in detail in the following subsections.

1) *Directional Embedding in Latent Sphere*: To extract semantically meaningful information from the input image,  $x$ , our watermarking agent,  $\theta$ , operates in the feature space of the CLIP image encoder [30], which is denoted as  $E_{\text{CLIP}}$ . Specifically, the feature vector  $f(x) = E_{\text{CLIP}}(x) \in \mathbb{R}^\zeta$  is L2-normalized, such that  $\|f(x)\|_2 = 1$ , constraining it to the surface of a  $\zeta$ -dimensional hypersphere. The watermarking agent has explicit control over the orthonormal embedding directions that it leverages to embed the message (i.e., watermark),  $M$ . However, allowing the watermarking agent to freely modify both the embedded message and the latent space directions makes it infeasible for the watermark extractor to recover the message without access to either the original image  $x$  or the watermark  $M$ . To address the challenge of extracting dynamically embedded messages, we propose deriving the latent space directions through a learnable **direction generator**,  $\mu$ , while relying on a **shared secret key**  $K$ . Specifically, the embedding directions are deterministically derived from  $K$ , which may be a password-like string. The key is first projected into the CLIP text embedding space [30] to obtain a feature vector  $f(K)$ . The direction generator network  $\mu$  then uses this feature to produce a canonical set of  $L$  orthonormal direction vectors  $D = \{d_1, d_2, \dots, d_L\}$ . Formally,

$$D = \mu(f(K)), \quad \text{where } d_i \in \mathbb{R}^d, \quad \|d_i\|_2 = 1 \quad (1)$$

Since  $D$  depends only on  $K$ , it remains consistent across all images. However, the directions are still **learnable**, as the weights  $\omega$  of  $\mu$  are optimised during training. For each bit  $m_i \in \{0, 1\}$  of a dynamically generated message  $M$ , the objective is to modify the image  $x$  to produce  $x'$  such that the projection of its new feature vector  $f(x')$  onto each direction  $d_i$  matches a target value,

$$\langle f(x'), d_i \rangle \approx p_i^{\text{target}} = \begin{cases} \xi_1 & \text{if } m_i = 1 \\ \xi_0 & \text{if } m_i = 0 \end{cases} \quad (2)$$

where  $\langle \cdot, \cdot \rangle$  denotes the dot product, and  $\xi_1, \xi_0$  are predefined projection magnitudes that encode binary values.

2) *Perturbative Watermark Embedding*: Once the  $m_i \in \{0, 1\}$  of the message  $M$  have been identified, the watermarking agent employs a MLP layer,  $\phi$ , that receives semantic features,  $f(x)$ , of  $x$  and the watermark,  $M$ , and synthesizes a perturbation map  $p$  over  $\zeta$ -dimensional feature vector  $f(x)$  such that:

$$q = \phi(x, M). \quad (3)$$

A decoder  $\pi$  then reconstructs the watermarked image  $x'$  from the perturbed features:

$$x' = \pi(q). \quad (4)$$

The watermarking agent's objective is to minimize a composite loss function  $\mathcal{L}_W$  that balances imperceptibility ( $\mathcal{L}_{\text{clip}}$ ), embedding accuracy ( $\mathcal{L}_{\text{dir}}$ ), and the conditional fragility objective ( $\mathcal{L}_{\text{ext}}$ ). Formally, this can be written as:

$$\mathcal{L}_W = \alpha \mathcal{L}_{\text{clip}} + \beta \mathcal{L}_{\text{dir}} + \gamma \mathcal{L}_{\text{ext}}, \quad (5)$$

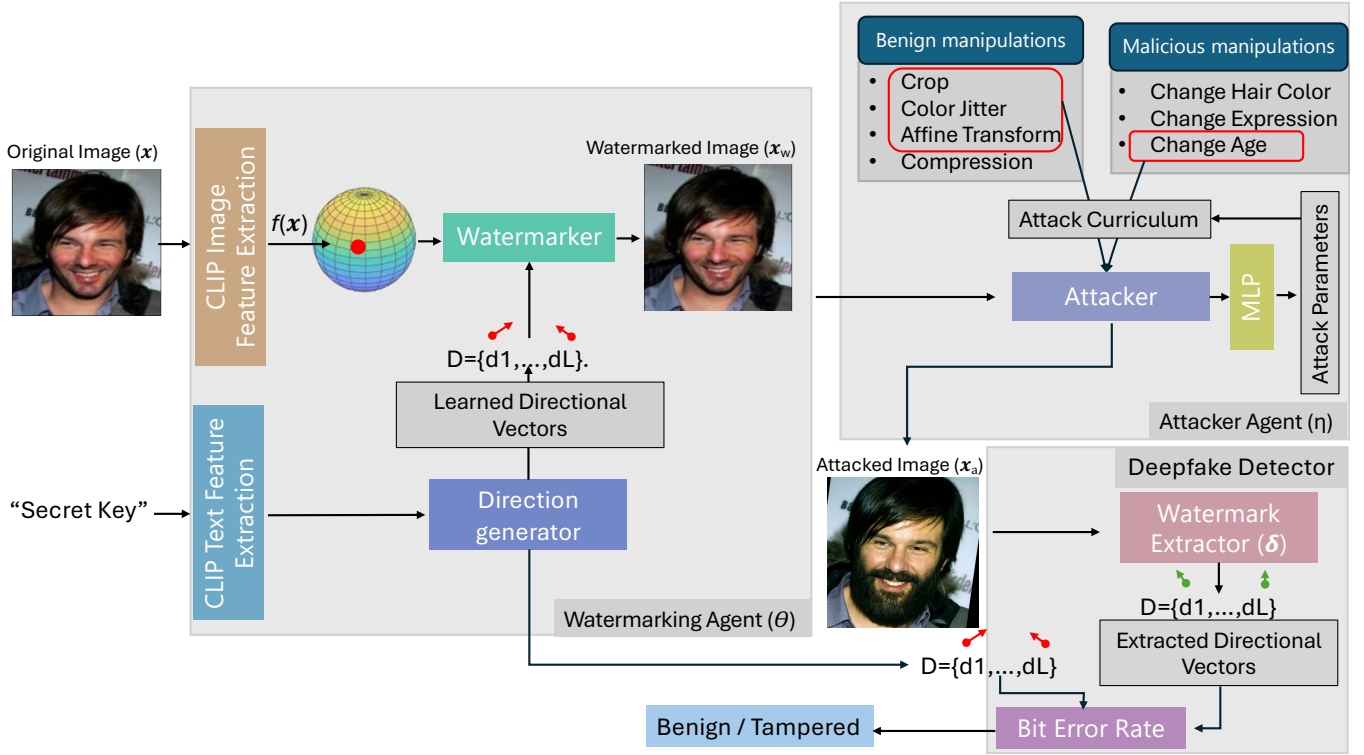


Fig. 2. Method Overview: Given an input image  $x$ , the watermarking agent  $\theta$  embeds a watermark  $w_x$  into the spherical latent space  $\mathbb{S}$  derived from semantic (CLIP Image) features  $f(x)$ , producing a watermarked image  $x_w$ . An attacker  $\eta$  generates an adversarial image  $x_a$  to disrupt watermark integrity.  $\eta$  uses both benign edits (e.g., JPEG compression, cropping) and semantic-altering manipulations (e.g., face swaps) when generating its attack curriculum. The extractor  $\delta$  attempts to recover  $w_x$  from any image  $x'$ ; failure to extract a valid watermark flags  $x'$  as a potential tampered image, leveraging watermark consistency as a proxy for semantic authenticity.

where,

$$\mathcal{L}_{\text{clip}} = \|f(x) - f(x')\|_2^2 \quad (6)$$

$$\mathcal{L}_{\text{dir}} = \text{CrossEntropy}(M, M'), \quad (7)$$

$$\mathcal{L}_{\text{ext}} = -\text{BER}(M, M'), \quad (8)$$

where  $M'$  is the recovered message obtained by decoding the projection vector  $P = \{\langle f(x'), d_i \rangle\}_{i=1}^L$  and  $\text{BER}(\cdot, \cdot)$  is Bit Error Rate. See Sec. III-D for details.

### C. Watermark Attacker

The objective of the watermark attacker,  $\eta$ , is to learn an optimal policy to destroy the embedded watermark. One of our key innovations is its ability to compose complex attacks using a predefined set of benign/traditional image transformations and malicious/generative transformations, effectively learning a dynamic attack curriculum which includes both type and intensity of each attack. The following subsections illustrate: (i) the process of composing a combinatorial attack, (ii) how the watermark attacker agent is trained, and (iii) how it is incentivized to identify attack curricula that lead to substantial semantic drifts and are closer to historically known failure regions in the latent space, where the watermark extractor fails to recover the watermark.

1) *Composing a Combinatorial Attack*: Let the set of available attacks, including the benign and malicious transformation, be denoted as  $\mathcal{A} = \{a_1, \dots, a_L\}$ . The watermark

attacker agent,  $\eta$ , receives the CLIP features,  $f(x')$ , of the watermarked image,  $x'$ , as input and outputs two vectors: logits for attack selection and normalized strength parameters  $\tau$  as:

$$(\text{logits}, \tau) = \eta(f(x')). \quad (9)$$

These logits are passed through a sigmoid function (denoted by  $\sigma$ ) to convert them into probabilities:

$$B = \sigma(\text{logits}) \in [0, 1]^L. \quad (10)$$

Then, for each probability,  $b_l$ , we sample a binary action,  $a_k$ , from a Bernoulli distribution as:

$$a_l \sim \text{Bernoulli}(P_l) \quad \forall l \in \{1, \dots, L\} \quad (11)$$

The result is a binary action vector  $a \in \{0, 1\}^L$  in which each element is independently sampled, creating a **combinatorial attack strategy**.

Simultaneously, the strength vector  $\tau \in [0, 1]^L$  determines the intensity for each attack. Each normalized value  $\tau_l$  is mapped to a meaningful parameter,  $\text{param}_l$ , in the selected attack type,  $a_l$ , and within a predefined range  $[\min_l, \max_l]$  as:

$$\text{param}_l = \min_l + (\max_l - \min_l) \cdot \tau_l. \quad (12)$$

2) *Learning an Attack Curriculum*: We train our watermark attacker agent using **reinforcement learning** to learn an optimal policy  $\psi$  that maximizes the likelihood of watermark extraction failure, thereby ensuring the success of the attack.

Specifically, the primary reward  $R$  for the watermark attacker agent can be formulated as the failure of the Watermark Extractor, measured by the Binary Cross-Entropy (BCE) loss between the extracted message  $\tilde{M}$  and the original message  $M$  as:

$$R_{\text{failure}} = \text{BCE}(\tilde{M}, M). \quad (13)$$

A strong and adaptive attack policy would drive the watermark to learn more resilient and sophisticated watermarking strategies. In contrast, the simplistic objective in Eq. 13, which focused solely on extractor failure, lacks the distinction required to drive meaningful improvements. As such, an advanced reward signal formulation is required to incentivize the attacker to pursue diverse and exploratory policies that provide richer adversarial signals.

3) *Promoting Semantic Drift and Targeted Shifts Toward Known Failure Regions:* We propose to augment the reward with bonuses to encourage exploration and exploitation. Specifically, we define a **curiosity reward** which is proportional to the squared Euclidean distance between the CLIP features of the image before and after the attack. This could be written as:

$$R_{\text{curiosity}} = \Delta \|f(x') - f(a(x'))\|^2, \quad (14)$$

where  $\Delta$  is a scaling factor. This reward incentivizes the attacker to discover attacks that cause the most significant semantic disruption, which are often the most challenging for a watermark to survive.

In addition, we introduce a **proximity reward** that encourages the attacker to perturb the image toward regions of the latent space known to challenge the watermark extractor. In particular, we introduce a memory buffer,  $J$ , that stores the latent representations,  $f(a(x'))$ , of images that have historically caused failures in watermark extraction. Then, the potential,  $\rho$ , of a new attacked image  $a(x'')$  can be defined as its proximity to its closest feature vector stored in the failure memory. Now the attacker’s proximity reward can be defined as inversely proportional to the distance of its attacked image from the closest failure memory embedding. Formally, this could be written as:

$$\begin{aligned} \rho(a(x'')) &= \min_{f_j \in J} \|f(a(x'')) - f_j\|_2, \\ R_{\text{proximity}} &= \frac{\nu}{\rho(a(x'')) + \epsilon}, \end{aligned} \quad (15)$$

where  $\nu$  is a scaling factor and  $\epsilon$  is a small constant to ensure numerical stability.

Now, the final loss function of the watermark attacker agent can be written as:

$$\mathcal{L}_\eta = -\mathbb{E}_{a \sim \phi} \left[ R_{\text{failure}} + R_{\text{proximity}} + R_{\text{curiosity}} + o \sum_{l=1}^L a_l \right] - r H(P) \quad (16)$$

where  $\sum_{l=1}^L a_l$  is a small regularization term penalizing the number of active actions,  $H(P)$  is the entropy of the action distribution  $P$ , and promotes exploration in the policy  $\phi$ ,

and  $o$  and  $r$  are hyperparameters. It should be noted that  $R_{\text{curiosity}}$  encourages goal-directed exploration while  $H(P)$  is used to encourage policy-level exploration such that the agent maintains diversity in action selection, serving complementary purposes in the learning process.

#### D. Watermark Extraction and Deepfake Detection

The watermark extractor,  $\delta$ , is responsible for recovering the message  $M$  from a potentially corrupted image  $x''$ . Specifically, given the input  $x''$ , it first extracts CLIP features  $f_{x''}$ , and independently generates the direction vectors,  $D$ , from the secret key,  $K$ , using the direction generator,  $\mu$ . Then it produces the projection of  $f_{x''}$  onto each of the direction vector  $d_i \in D$  as:

$$p_i'' = \langle f_{x''}, d_i \rangle. \quad (17)$$

The resulting vector of projections  $P'' = \{p_1'', \dots, p_L''\}$  is passed through an MLP, which outputs the logits for the predicted message,  $M'$ .

In the proposed framework, the fragility of the watermark serves as the deepfake detection mechanism. Even when the direction generator,  $\mu$ , the integrity of an input image can be verified at inference time by computing the Bit Error Rate (BER) between the extracted message  $M'$  and the known original message  $M$ . Since the same trained direction generator  $\mu$  and secret key  $K$  are used during both watermark embedding and extraction, the resulting direction vectors should remain consistent. A high BER indicates potential generative manipulation, enabling us to leverage the fragility of the watermark as a deepfake detection signal. Formally, this could be written as:

$$f_{\text{DEEPPFAKE}}(x'') = \begin{cases} \text{True}, & \text{if } \text{BER}(M', M) > \lambda \\ \text{False}, & \text{otherwise} \end{cases} \quad (18)$$

where  $\lambda$  is a predefined classification threshold.

#### E. Implementation Details

Implementation of this framework is completed using PyTorch. All the images are resized to a resolution of  $224 \times 224$ . For both watermarking agent and attacker agent, Adam [31] optimiser with a learning rate of  $1e^{-4}$  is used for optimisation. The model is trained for 50 epochs with a batch size of 16 on an NVIDIA A100 GPU. For consistency in comparison, similar to baseline methods, the length of the watermark bits is set to 512 bits. The classification threshold,  $\lambda$  is evaluated experimentally and set to 0.8. The architecture details of the watermarking agent, watermark attacker, direction generator, and watermark extractor are provided below.

The Direction Generator ( $\mu$ ) receives the 512-D CLIP-Text feature of the secret message. This is processed by a two-layer MLP: a linear layer of 256 dimensions followed by ReLU, and a second linear layer ( $\mathbb{R}^{256} \rightarrow \mathbb{R}^{512}$ ). The output is L2-normalized along the feature dimension.

The watermarker operates in the CLIP feature space. It combines the original CLIP image feature (512 dimensions) and the directional vectors (512 dimensions) into a 1024-D vector. This is processed by a linear layer with 512 hidden

units and ReLU activation, and outputs a 512-D feature-space perturbation using Tanh activation, which is then passed to the integrated Image Decoder. The decoder,  $\pi$ , first maps this vector to a higher-dimensional space using a single FC layer ( $\mathbb{R}^{512} \rightarrow \mathbb{R}^{4096}$ ), reshaping the output to  $256 \times 4 \times 4$ . This tensor is sequentially upsampled through five transposed convolutional layers, using ReLU (except the final layer’s Tanh) and a stride of 2 (except for the final layer’s stride of 4) to reach the final  $3 \times 224 \times 224$  image resolution.

The watermark extractor ( $\delta$ ) recovers the message by first projecting the 512-D CLIP features onto a 128-D latent space. This vector is then passed through a two-layer MLP: a linear layer ( $\mathbb{R}^{128} \rightarrow \mathbb{R}^{256}$ ) with ReLU, followed by a final linear layer ( $\mathbb{R}^{256} \rightarrow \mathbb{R}^{512}$ ) to output the message logits.

The watermark attacker ( $\eta$ ) uses a shared two-layer MLP backbone, first layer with 256 hidden units and ReLU activation, and the next layer with 128 hidden units and ReLU activation. This backbone outputs two vectors: a vector of logits for attack selection, and a vector of normalized strength parameters. The logits are passed through a Sigmoid function to yield a probability vector,  $B$ . For each probability  $b_l$ , a binary action  $a_l$  is sampled from a Bernoulli( $P_l$ ) distribution, resulting in a binary action vector  $a \in \{0, 1\}^L$  that defines the combinatorial attack strategy. The strength vector  $\tau$  determines the intensity for each attack.

#### IV. EXPERIMENTS

In this section, we present the results of our experiments designed to evaluate and compare the effectiveness of the proposed DeepForgeSeal framework against existing state-of-the-art methods. We begin by detailing the datasets used in our evaluations (Sec. IV-A), followed by a description of the evaluation metrics employed to assess model performance (Sec. IV-B). The main experimental results, where we benchmark our method against current state-of-the-art approaches, are provided in Sec. IV-C. Additionally, ablation studies conducted to validate the contributions of the learnable directional embedding strategy, adversarial learning pipeline, and novel reward function are discussed in Sec. IV-D. Finally, we analyse the time complexity of the DeepForgeSeal model in Sec. IV-E.

##### A. Datasets

Following prior works [6], we use Flickr-Faces-HQ (FFHQ) [32] dataset for training our model, and CelebA [33] and CelebA-HQ [34] datasets for evaluating the model and demonstrating its generalisability. The FFHQ dataset contains 70,000 images at a resolution of  $1024 \times 1024$  pixels. In accordance with the dataset authors’ guidelines, the first 60,000 images are designated for training, while the remaining 10,000 are reserved for validation. We follow this protocol and use the training subset of FFHQ to train our model. CelebA comprises 10,000 distinct identities, with each identity represented by 20 images at a  $128 \times 128$  resolution. CelebA-HQ is a high-quality version of the CelebA dataset, consisting of 30,000 images at a resolution of  $1024 \times 1024$  pixels. Specifically, we followed the official test split provided by the CelebA and CelebA-HQ dataset authors to enable direct comparisons.

##### B. Evaluation Metrics

We evaluate our method from two key perspectives. First, we assess the visual fidelity of the watermarked images compared to the original images using two widely adopted metrics: Peak Signal-to-Noise Ratio (PSNR) and Structural Similarity Index Measure (SSIM). PSNR provides a quantitative measure of the pixel-level differences, where higher values indicate less distortion and better preservation of image quality. SSIM, on the other hand, evaluates perceptual similarity by considering factors such as luminance, contrast, and structural information, offering a more human-aligned assessment of image quality. Together, these metrics help us determine how effectively our method maintains the integrity of the original image while embedding the watermark.

To evaluate the performance of deepfake detection, following prior works [6], we compute image-level Accuracy (ACC) and F1-Score. Accuracy reflects the overall proportion of correctly classified images, encompassing both correctly identified real and fake samples. The F1-Score, which balances precision and recall, is particularly informative in capturing the trade-off between false alarms (incorrectly classifying real images as fake) and miss detections (failing to identify fake images). Together, these metrics provide a reliable measure of the system’s ability to detect deepfakes while minimizing classification errors.

##### C. Comparisons with Existing State-of-the-art Methods

In this section, we report results for the proposed model and compare with the existing state-of-the-art methods considering the visual quality of the watermarking (See Sec. IV-C1), deepfake detection performance (See Sec. IV-C2), and watermark’s resilience and fragility (See Sec. IV-C3).

1) *Visual Quality of Watermarking Approaches*: As baselines we use state-of-the-art methods, including FaceSigns [19], EditGard [10], and Zhao et. al [6]. When choosing our baselines, we ensured that a variety of different deep learning approaches, including adversarial trained models [19], dual-purpose watermarking methods for tamper detection and copyright protection [10], and identity-entangled watermarking methods [6], are compared, enabling a comprehensive comparison.

TABLE I  
VISUAL FIDELITY OF DIFFERENT WATERMARKING TECHNIQUES. THE BEST RESULTS ARE HIGHLIGHTED IN BOLD.

Model	Quality Metrics	
	PSNR ( $\uparrow$ )	SSIM ( $\uparrow$ )
FaceSigns [19]	32.03	0.92
Zhao et. al [6]	38.32	0.94
EditGard [10]	45.07	0.96
DeepForgeSeal (ours)	<b>48.39</b>	<b>0.97</b>

Quantitative comparisons for the CelebA-HQ dataset are presented in Tab. I. When comparing the proposed DeepForgeSeal with the previous state-of-the-art methods, we observe that our method has the highest PSNR and SSIM, demonstrating our framework’s ability to embed watermarks stealthily, preserving the image’s visual quality. We attribute this to

operating within the high-dimensional semantic space of the input images, which enables subtle yet effective modifications.

In addition to the above quantitative comparisons, in Fig. 3 we present a qualitative comparison between FaceSigns [19], EditGard [10], and the proposed DeepForgeSeal method for embedding watermarks in two sample images from the CelebA dataset. Figure 3 supports the findings from our quantitative comparisons, showing that our watermarked images maintain high visual realism by accurately preserving the original textures, hue, and lighting. In contrast, both FaceSigns and EditGuard noticeably alter the image hue, with FaceSigns additionally introducing visible artefacts in the facial region. These results highlight the effectiveness of our proposed framework, which embeds watermarks in the latent space rather than directly in the pixel space, enabling more natural and less intrusive modifications.

2) *Deepfake Detection Performance*: We compare the proposed DeepForgeSeal method with both passive and proactive deepfake detection methods. Following [6], we employ CelebA and CelebA-HQ datasets to represent low and high-resolution real image cases and generate deepfakes using a variety of deepfake generation methods, including AttGAN, StarGAN, InfoSwap and SimSwap, CIAGAN, and DeepPrivacy. These methods allow us to evaluate the performance of the proposed deepfake detection framework against a wide range of malicious manipulations, including identity swapping and face anonymization techniques. In our experimental pipeline, for passive deepfake detection methods, we use non-watermarked images from the CelebA and CelebA-HQ datasets as real images. The above deepfake generation techniques are then applied to create their fake counterparts. For proactive deepfake detection methods, including the proposed DeepForgeSeal approach, we first watermark the images from the CelebA and CelebA-HQ datasets, and then generate the corresponding fake images using the same deepfake generation methods.

Following [6], as baselines for passive deepfake detection we use the state-of-the-art BTS [35], CD [36], Bonettini et. al [37], PF [38], RFM [39], SBI [40], and CBO-DD [41]. In addition, the state-of-the-art FaceSigns [19], EditGard [10], and Zhao et al. [6], which are proactive deepfake detection methods, have also been used for comprehensiveness.

Tab. II summarises the comparison results for deepfake detection in CelebA and CelebA-HQ datasets. It is evident that passive deepfake detection methods generally struggle to generalise across different deepfake generation techniques. Among the approaches evaluated, only methods such as SBI [40] and CBO-DD [41] consistently demonstrate strong performance across all considered generation methods. In contrast, most other passive detection techniques perform well against a limited subset of generation methods but show significant performance degradation when applied to others. This limitation stems from their training approach, which focuses on identifying artefacts specific to the generation techniques used during training. Consequently, these methods tend to perform poorly when tested on deepfakes produced by unfamiliar or diverse generation techniques.

When comparing the results of the proactive detection

methods FaceSigns [19], Zhao et. al [6], and EditGard [10] with the proposed DeepForgeSeal method, we see that our method has been able to achieve significant detection accuracy across all considered generation methods. Although state-of-the-art methods such as Zhao et. al [6], and EditGard [10] have been able to achieve impressive performance against deepfake generation methods such as AttGAN and DeepPrivacy, their performance degrade when tested against DeepPrivacy and StarGAN2 generation methods. In contrast, our proposed DeepForgeSeal method consistently demonstrates superior detection performance across all evaluated deepfake generation techniques. We attribute this to the learnable watermarking strategy embedded within the framework, which enables explicit control over message encoding and extraction. Additionally, the adversarial reinforcement learning pipeline allows the watermarking agent to actively observe and respond to malicious attacks, dynamically adapting its watermarking strategy. Together, these components contribute to DeepForgeSeal’s strong generalisation capability across a wide range of deepfake generation methods.

To further demonstrate the strong generalisation capabilities of the proposed method, we conducted an additional evaluation involving a series of facial attribute manipulations and face reenactments using watermarked images. For this experiment, we employed several state-of-the-art generative AI (GenAI) video synthesis tools, including OpenAI SORA, Gemini Veo 3, StyleMask, and Hyper Reenact, and tested the deepfake detection performance of our DeepForgeSeal approach using these manipulated images. It is important to note that the DeepForgeSeal model was not exposed to these types of manipulations during training. Fig 4 presents qualitative visualisations, highlighting the faces our method successfully identified as fake. For video-level decisions, we computed the average of frame-level detection scores. As anticipated, our model effectively detected manipulations generated by the latest GenAI video synthesis tools, demonstrating its robustness and ability to provide comprehensive protection against malicious deepfakes. For additional visual examples, please refer to the supplementary material.

### 3) *Watermark Resilience and Fragility Against Attacks*:

In this section, we compare the resilience of our DeepForgeSeal watermarking methods with the current state-of-the-art methods under different attacks against watermarks. For comprehensiveness, we consider both traditional benign attacks, such as cropping, compression, and color changes, as well as the learnable benign attacks proposed by Zhao et. al [42] and Lukas et. al [43]. In addition, to quantitatively assess the fragility against malicious image manipulations, we generate attacks using state-of-the-art GAN-based face swapping and reenactment techniques, including SimSwap [44], UniFace [45], FaceDancer [46], and HyperReenact [47].

The evaluation results are presented in Tab. III. As baselines, we use the state-of-the-art FaceSigns [19] and EditGard [10] semi-fragile watermarking methods. Following prior works [19], [10], we measure the Bit Recovery Accuracy (BRA) as the evaluation metric, where we expect a higher BRA against benign and lower BRA against malicious transforms to achieve the goal of semi-fragile watermarking. As reported

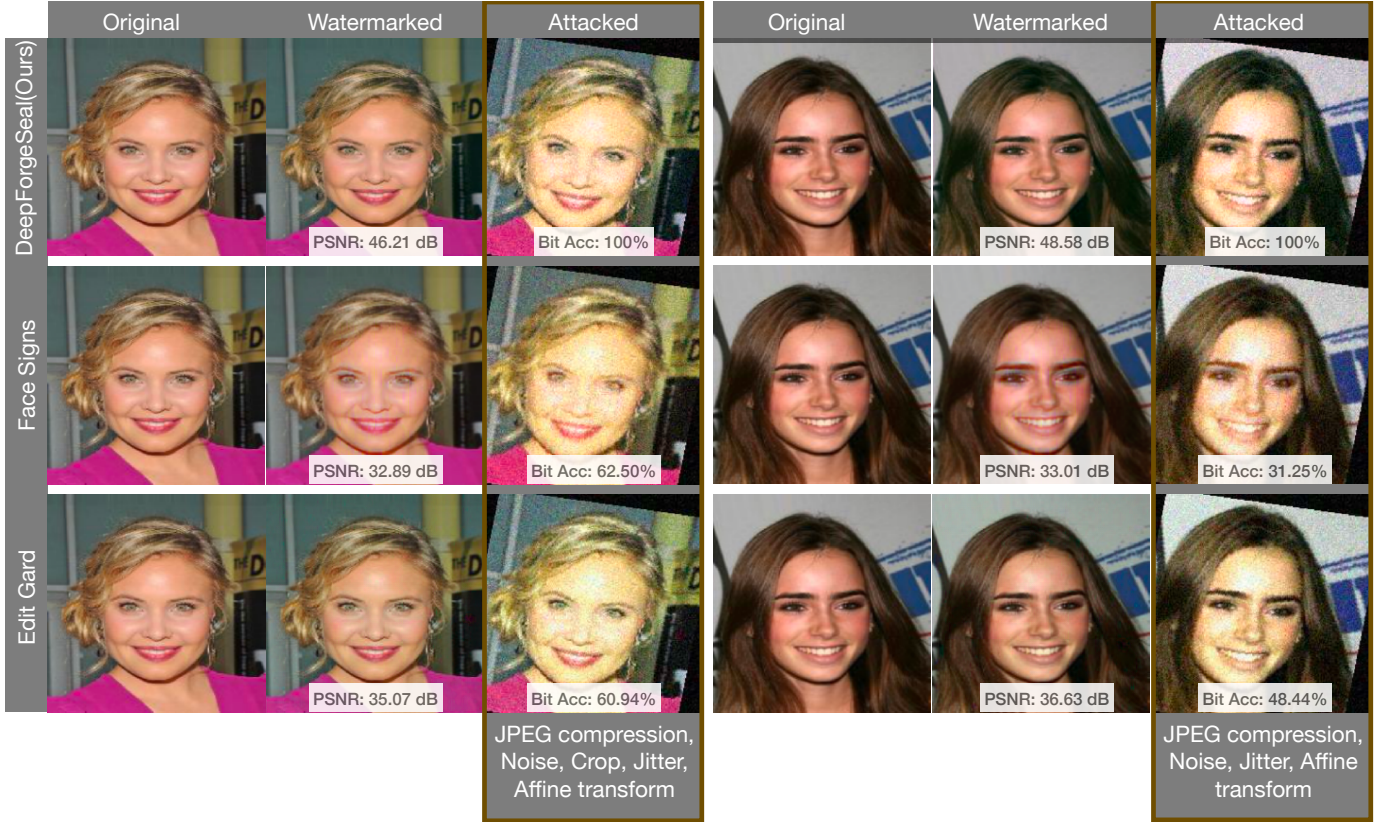


Fig. 3. Qualitative Results of Visual Quality: A comparison between the existing state-of-the-art models, FaceSigns [19], EditGard [10], and the proposed DeepForgeSeal method for watermarking two sample images from the CelebA dataset [33].

TABLE II  
ACCURACY ( $\uparrow$ ) AND F1 SCORES ( $\uparrow$ ) OF DIFFERENT METHODS' DEEPFAKE DETECTION RESULTS. THE BEST RESULTS ARE HIGHLIGHTED IN BOLD.

Detection methods	Low Resolutions (CelebA)						High Resolutions (CelebA-HQ)					
	AttGAN	CIAGAN	DeepPrivacy	InfoSwap	SimSwap	StarGAN2	AttGAN	CIAGAN	DeepPrivacy	InfoSwap	SimSwap	StarGAN2
BTS [35]	0.86/0.87	0.51/0.66	0.50/0.66	0.49/0.66	0.51/0.67	0.53/0.67	0.86/0.87	0.50/0.66	0.50/0.66	0.49/0.65	0.50/0.66	0.55/0.68
CD [36]	0.88/0.86	0.51/0.03	0.51/0.01	0.54/0.17	0.51/0.01	0.78/0.71	0.81/0.77	0.51/0.04	0.52/0.07	0.52/0.07	0.52/0.06	0.84/0.81
Bonettini et. al [37]	0.59/0.69	0.62/0.62	0.58/0.68	0.57/0.64	0.60/0.71	0.63/0.63	0.53/0.68	0.65/0.62	0.56/0.69	0.51/0.66	0.55/0.69	0.49/0.65
PF [38]	0.76/0.79	0.51/0.66	0.52/0.65	0.57/0.68	0.54/0.67	0.99/0.98	0.75/0.79	0.51/0.66	0.55/0.68	0.56/0.69	0.54/0.68	<b>0.98/0.97</b>
RFM [39]	0.50/0.67	0.51/0.67	0.51/0.67	0.50/0.67	0.51/0.67	0.50/0.67	0.50/0.67	0.50/0.67	0.51/0.67	0.50/0.67	0.50/0.67	0.50/0.67
SBI [40]	0.79/0.82	0.77/0.8	0.78/0.82	0.77/0.81	0.78/0.81	0.72/0.75	0.80/0.80	0.72/0.78	0.78/0.80	0.76/0.77	0.83/0.84	0.69/0.70
CBO-DD [41]	0.84/0.84	0.91/0.93	0.86/0.87	0.79/0.85	0.84/0.88	0.85/0.85	0.83/0.86	0.92/0.93	0.86/0.87	0.80/0.85	0.89/0.91	0.82/0.84
FaceSigns [19]	0.91/0.93	0.83/0.84	0.91/0.95	0.93/0.95	0.95/0.95	0.96/0.98	0.87/0.88	0.92/0.93	0.80/0.83	0.91/0.91	0.82/0.82	0.84/0.87
Zhao et. al [6]	0.94/0.94	0.87/0.86	0.98/0.98	0.98/0.98	0.97/0.98	0.82/0.84	0.94/0.94	0.85/0.82	0.99/0.98	<b>0.99/0.99</b>	0.98/0.98	0.85/0.87
EditGard [10]	0.96/0.97	0.88/0.88	0.96/0.98	0.94/0.97	0.97/0.98	0.91/0.93	0.95/0.96	0.87/0.91	0.97/0.99	<b>0.99/0.99</b>	0.98/0.99	0.93/0.95
<b>DeepForgeSeal (Ours)</b>	<b>0.96/0.98</b>	<b>0.92/0.95</b>	<b>0.99/0.99</b>	<b>0.98/0.99</b>	<b>0.98/0.98</b>	<b>0.99/0.99</b>	<b>0.96/0.98</b>	<b>0.95/0.96</b>	<b>0.99/0.99</b>	<b>0.99/0.99</b>	<b>0.99/0.99</b>	<b>0.98/0.97</b>

TABLE III  
BIT RECOVERY ACCURACY (BRA) OF BASELINE FACE SIGNS [19] AND EDITGARD [10] WATERMARKING METHODS AND PROPOSED DEEPFORGESEAL METHOD UNDER BENIGN AND MALICIOUS TRANSFORMATIONS. THE BEST RESULTS ARE HIGHLIGHTED IN BOLD.

Method	BRA (%) - Benign Transforms ( $\uparrow$ )						BRA (%) - Malicious Transforms ( $\downarrow$ )				
	JPG	Noise	Crop	Jitter	Affine	Zhao et. al [42]	Lukas et. al [43]	SimSwap	UniFace	FaceDancer	HyperReenact
FaceSigns [19]	0.87	0.73	0.72	0.91	0.96	0.87	0.88	0.52	0.49	0.62	0.51
EditGard [10]	0.95	0.78	0.96	0.96	0.99	0.92	0.95	0.48	0.49	0.44	0.50
<b>DeepForgeSeal (ours)</b>	<b>1.00</b>	<b>0.98</b>	<b>0.98</b>	<b>0.99</b>	<b>1.00</b>	<b>0.98</b>	<b>0.99</b>	<b>0.24</b>	<b>0.11</b>	<b>0.10</b>	<b>0.06</b>



Fig. 4. Qualitative results of our DeepForgeSeal model when tested on videos generated by completely unseen image and video deepfake generation techniques (OpenAI SORA, Gemini Veo 3, StyleMask, and Hyper Reenact). We visualise the sample images showing the detected face, along with the original (bonafide) watermarked image before the manipulation (provided in bottom left). For additional visualisations, please refer to the supplementary material.

in Tab. III, we observe that both baseline models perform poorly against benign image manipulations, demonstrating that these watermarking techniques are too fragile to withstand the benign image transformations that users can apply in the real world. At the same time, both baseline techniques demonstrate less fragility towards the malicious, content-altering manipulations that the considered face swapping and reenactment techniques have generated. These evaluations clearly demonstrate the limitations of the existing state-of-the-art watermarking techniques and the superiority of the DeepForgeSeal paradigm that enables us to learn a strategy that optimally balances watermark resilience and fragility.

#### D. Ablation Evaluations

We conducted a series of ablation studies to systematically analyse the impact of the individual innovations that our DeepForgeSeal framework proposes. Several design choices contribute to the robustness of our model: i) the proposed

learnable directional embedding strategy that uses a latent sphere; ii) the proposed adversarial learning pipeline with composed attacks with a learnable attack curriculum; and iii) the novel reward function that promotes semantic drift and targeted shifts toward known failure regions. All ablation experiments were conducted on the CelebA-HQ dataset, and for testing the ablation models, we used the validation set of CelebA-HQ. As evaluation metrics, we use PSNR and average BRA against benign and malicious manipulations.

1) *Effects of Learnable Directional Embedding in Latent Sphere:* To study the effect of the proposed learnable directional embedding strategy that uses a latent sphere, we generated two ablation variants of the proposed DeepForgeSeal model: i) DeepForgeSeal - w/o [D] - a model with naive latent embedding in which we embed the message directly in the latent space without directional encoding, and ii) DeepForgeSeal - FD - a model with fixed directional embeddings.

Results of this comparison are shown in Tab. IV. We observe

TABLE IV  
EFFECT OF LEARNABLE DIRECTIONAL EMBEDDING IN LATENT SPHERE.  
THE BEST RESULTS ARE HIGHLIGHTED IN BOLD.

Model	PSNR ( $\uparrow$ )	BRA - Benign ( $\uparrow$ )	BRA - Malicious ( $\downarrow$ )
DeepForgeSeal - w/o [D]	48.43	0.78	0.42
DeepForgeSeal - FD	46.58	0.86	0.19
DeepForgeSeal	<b>48.12</b>	<b>0.99</b>	<b>0.12</b>

that the learnable directional embedding strategy is an integral part of the proposed framework. Specifically, we observe that the naive latent embedding approach, where the message is directly embedded into the latent space, leads to a reduction in PSNR, distorts the natural image characteristics, and diminishes the watermark’s resilience against benign image transformations. The introduction of directional embedding enhances the robustness of the watermark (see the row corresponding to DeepForgeSeal - FD). Notably, the experimental results demonstrate that the learnable directional embedding strategy, which encodes the message within a latent sphere, achieves the most favorable balance between resilience and fragility, while preserving image fidelity. These experiments confirm the utility of our learnable directional embedding procedure.

2) *Effects of Composing a Combinatorial Attack and Learning an Attack Curriculum*: The effectiveness of the proposed adversarial learning pipeline with composed attacks with a learnable attack curriculum is evaluated in this experiment. We generated eight ablation variants of the proposed DeepForgeSeal model: i) DeepForgeSeal - w/o  $\eta$  - a model without a watermark attacker agent, ii) DeepForgeSeal - w/o  $\mathcal{A}$  - a model in which one fixed attack type (no composition or learning of an attack curriculum) is applied, iii) DeepForgeSeal -  $|\mathcal{A}|$  - a model in which multiple attacks are applied in a fixed sequence, iv) DeepForgeSeal -  $\tilde{\mathcal{A}}$  - a model in which multiple random combinations of attacks applied, v) DeepForgeSeal -  $a_1, \tau^\uparrow$  - a model in which a single attack type with gradually increasing strength is applied, vi) DeepForgeSeal -  $\mathcal{A}^\rightarrow$  - a model which progressively introduces more complex combinations of attacks, vii) DeepForgeSeal -  $a_1, \tau$  - a model with single attack type with learnable strength parameter, viii) DeepForgeSeal -  $[\mathcal{A}]$  - a model with a predefined attack curriculum without adaptation to agent performance.

TABLE V  
EFFECTS OF COMPOSING A COMBINATORIAL ATTACK AND LEARNING AN ATTACK CURRICULUM. THE BEST RESULTS ARE HIGHLIGHTED IN BOLD.

Model	PSNR ( $\uparrow$ )	BRA - Benign ( $\uparrow$ )	BRA - Malicious ( $\downarrow$ )
DeepForgeSeal - w/o $\eta$	32.11	0.61	0.59
DeepForgeSeal - w/o $\mathcal{A}$	41.58	0.72	0.55
DeepForgeSeal - $ \mathcal{A} $	46.20	0.82	0.37
DeepForgeSeal - $\tilde{\mathcal{A}}$	47.15	0.87	0.31
DeepForgeSeal - $a_1, \tau^\uparrow$	47.12	0.76	0.42
DeepForgeSeal - $\mathcal{A}^\rightarrow$	48.09	0.92	0.22
DeepForgeSeal - $a_1, \tau$	48.05	0.79	0.38
DeepForgeSeal - $[\mathcal{A}]$	47.11	0.89	0.28
DeepForgeSeal	<b>48.12</b>	<b>0.99</b>	<b>0.12</b>

From the results in Tab. V, we can confirm that there are benefits to incorporating both combinatorial attacks with a learnable attack curriculum as an adversary in the proposed framework, which is evidenced by the rows in Tab. V corresponding to models DeepForgeSeal -  $\mathcal{A}^\rightarrow$ , and DeepForgeSeal -  $a_1, \tau$ . Most importantly, when the attacker agent has the

knowledge of the current vulnerabilities of the victim model (i.e. watermarking agent), it helps the attacker dynamically adapt its strategy and generate a more complex curriculum of attacks, in turn helping the victim to understand the vulnerabilities of its watermarking strategy and rectifying those. We believe this is the reason for the poor performance of the DeepForgeSeal -  $[\mathcal{A}]$  model, in which a predefined attack curriculum was used without adaptation to the victim’s performance. Furthermore, rows corresponding to DeepForgeSeal -  $|\mathcal{A}|$ , and DeepForgeSeal -  $\tilde{\mathcal{A}}$  confirm the importance of using a combinatorial attack in which a learnable agent determines the attack sequence. Therefore, using this experiment, we can confirm the necessity of both combinatorial attacks and learning an attack curriculum to enhance the robustness of the watermark, while simultaneously preserving image fidelity.

3) *Effects of Promoting Semantic Drift and Targeted Shifts Toward Known Failure Regions*: To better establish the contributions of the proposed reward function that promotes semantic drift and targeted shifts toward known failure regions, we conducted a further ablation experiment. Specifically, three ablation variants of the proposed model were generated: i) DeepForgeSeal - w/o  $[R_{\text{proximity}}, R_{\text{curiosity}}]$  - proposed model without both curiosity reward and proximity reward, ii) DeepForgeSeal - w/o  $R_{\text{proximity}}$  - proposed model with curiosity reward but without proximity reward, iii) DeepForgeSeal - w/o  $R_{\text{curiosity}}$  - proposed model without curiosity reward but with proximity reward.

TABLE VI  
EFFECTS OF THE PROMOTING SEMANTIC DRIFT AND TARGETED SHIFTS TOWARD KNOWN FAILURE REGIONS. THE BEST RESULTS ARE HIGHLIGHTED IN BOLD.

Model	PSNR ( $\uparrow$ )	BRA - Benign ( $\uparrow$ )	BRA - Malicious ( $\downarrow$ )
DeepForgeSeal - w/o $[R_{\text{proximity}}, R_{\text{curiosity}}]$	48.10	0.82	0.35
DeepForgeSeal - w/o $R_{\text{proximity}}$	48.12	0.91	0.24
DeepForgeSeal - w/o $R_{\text{curiosity}}$	48.08	0.94	0.21
DeepForgeSeal	<b>48.12</b>	<b>0.99</b>	<b>0.12</b>

The results presented in Tab. VI confirm the need for the proposed innovative reward function. In particular, the ablation model without both the multi-head retrieval mechanism and the dynamic masking procedure (see the row corresponding to DeepForgeSeal - w/o  $[R_{\text{proximity}}, R_{\text{curiosity}}]$  in Tab. VI) struggles to achieve a good watermark robustness. This is because the attacker agent has learned a sub-optimal attacking policy, marking the watermarking agent unprepared for real-world attacks against watermarks. Comparing rows corresponding to DeepForgeSeal - w/o  $R_{\text{proximity}}$  and DeepForgeSeal - w/o  $R_{\text{curiosity}}$  models in Tab. VI, we can confirm that proximity and curiosity rewards complement each other. By leveraging underexplored regions of the latent space alongside known failure zones encountered during watermark retrieval, the attacker agent can formulate a sophisticated attack policy. This, in turn, drives the watermarker agent to refine and strengthen its watermarking strategy. These observations strongly validate the importance of the proposed reward function that promotes semantic drift and targeted shifts toward known failure regions

### E. Time Complexity

We perform a detailed time complexity analysis using two state-of-the-art watermarking techniques: FaceSigns [19] and

EditGard [10]. These methods were selected due to the public availability of their implementations. Using a single NVIDIA A100 GPU, we measured the average time required to generate 100 image-level predictions, including preprocessing, feature extraction, watermark extraction, and deepfake classifications. The results of this analysis are summarized in Table VII.

Model	Total Params (M)	Runtime (in Sec)
FaceSigns [19]	7.58	7.1205
EditGard [10]	9.32	8.6201
DeepForgeSeal (Ours)	8.27	7.8535

TABLE VII  
TIME COMPLEXITY ANALYSIS: THE PARAMETER COUNT IN MILLIONS AND THE TIME TAKEN TO GENERATE 100 IMAGE-LEVEL PREDICTIONS USING A SINGLE NVIDIA A100 GPU

## V. CURRENT LIMITATIONS AND FUTURE DIRECTIONS

We observe two limitations of DeepForgeSeal: (i) The proposed system has been developed for watermarking image data and has not yet been tested for multimodal data or other modalities such as audio data. Given the growing prevalence of multimodal deepfakes, it is crucial to assess the applicability of the proposed learnable watermarking strategy, particularly its use of high-dimensional semantic spaces, multi-agent adversarial reinforcement learning, and innovative reward functions, for other data types. Future research could also focus on extending this framework to support multimodal watermarking. One promising direction would be to design a more sophisticated multi-agent architecture that facilitates collaboration among watermarking agents. Such a system could more effectively navigate and exploit the multimodal latent space, enhancing semantic stealth and robustness across diverse modalities. (ii) While our evaluations (Tab. VII) indicate that the proposed model exhibits computational complexity comparable to existing state-of-the-art watermarking systems, it has not been tested on resource-constrained environments such as edge devices (e.g., smartphones). The reliance on high-dimensional semantic embeddings and multi-agent interactions increases the computational demands, potentially limiting scalability and real-time performance. To address these limitations, future research could explore model compression techniques such as pruning, quantization, or knowledge distillation. These strategies may help reduce inference time and memory footprint while preserving detection accuracy, thereby improving the feasibility of deploying the DeepForgeSeal model in edge scenarios.

## VI. CONCLUSION

This paper presented *DeepForgeSeal*, a Latent Space-Driven Semi-Fragile Watermarking using Multi-Agent Adversarial Reinforcement Learning (MAARL) for accurate detection of face deepfakes. We demonstrate that the proposed learnable watermarking agent achieves enhanced robustness and semantic stealth through a directional embedding strategy in the latent space. The MAARL paradigm enabled the agent to dynamically balance resilience and fragility by interacting with a

curriculum of benign and adversarial manipulations introduced by an attacker agent. To intensify this adversarial interaction, we designed reward functions that encouraged semantic drift and targeted perturbations toward known failure regions. This incentivised the attacker agent to develop sophisticated attack strategies, which in turn drove the watermarking agent to refine and strengthen its embedding approach, resulting in a more resilient and adaptive watermarking system. Extensive experiments were conducted on two public benchmarks: CelebA and CelebA-HQ, which demonstrated the ability of the proposed framework to outperform the current state-of-the-art algorithms by significant margins.

## ACKNOWLEDGMENT

The research was supported by the Australian Government through the Office of National Intelligence Postdoctoral Grant awarded to the primary author under Project NIPG-2024-022.

## REFERENCES

- [1] T. Hunter, "Princess catherine cancer video spawns fresh round of ai conspiracies," 2024, accessed on 31 09, 2025. [Online]. Available: <https://www.washingtonpost.com/technology/2024/03/27/kate-middleton-video-cancer-ai/>
- [2] W. Galston, "Is seeing still believing? the deepfake challenge to truth in politics," 2020, accessed on 09 23, 2025. [Online]. Available: <https://www.brookings.edu/articles/is-seeing-still-believing-the-deepfake-challenge-to-truth-in-politics/>
- [3] N. S. Agenc, "Nsa, u.s. federal agencies advise on deepfake threats," 2023, accessed on 08 23, 2025. [Online]. Available: <https://www.nsa.gov/Press-Room/Press-Releases-Statements/Press-Release-View/Article/3523329/nsa-us-federal-agencies-advise-on-deepfake-threats/>
- [4] T. Fernando, D. Priyasad, S. Sridharan, A. Ross, and C. Fookes, "Face deepfakes—a comprehensive review," *arXiv preprint arXiv:2502.09812*, 2025.
- [5] M. Mustak, J. Salminen, M. Mäntymäki, A. Rahman, and Y. K. Dwivedi, "Deepfakes: Deceptions, mitigations, and opportunities," *Journal of Business Research*, vol. 154, p. 113368, 2023.
- [6] Y. Zhao, B. Liu, M. Ding, B. Liu, T. Zhu, and X. Yu, "Proactive deepfake defence via identity watermarking," in *Proceedings of the IEEE/CVF winter conference on applications of computer vision*, 2023, pp. 4602–4611.
- [7] T. Wang, H. Cheng, M.-H. Liu, and M. Kankanhalli, "Fractalforensics: Proactive deepfake detection and localization via fractal watermarks," *arXiv preprint arXiv:2504.09451*, 2025.
- [8] X. Wu, X. Liao, and B. Ou, "Sepmark: Deep separable watermarking for unified source tracing and deepfake detection," in *Proceedings of the 31st ACM International Conference on Multimedia*, 2023, pp. 1190–1201.
- [9] X. Zhang, Z. Tang, Z. Xu, R. Li, Y. Xu, B. Chen, F. Gao, and J. Zhang, "Omniguard: Hybrid manipulation localization via augmented versatile deep image watermarking," in *Proceedings of the Computer Vision and Pattern Recognition Conference*, 2025, pp. 3008–3018.
- [10] X. Zhang, R. Li, J. Yu, Y. Xu, W. Li, and J. Zhang, "Editguard: Versatile image watermarking for tamper localization and copyright protection," in *Proceedings of the IEEE/CVF conference on computer vision and pattern recognition*, 2024, pp. 11 964–11 974.
- [11] A. Haliassos, K. Vougioukas, S. Petridis, and M. Pantic, "Lips don't lie: A generalisable and robust approach to face forgery detection," in *Proceedings of the IEEE/CVF conference on computer vision and pattern recognition*, 2021, pp. 5039–5049.
- [12] S. Agarwal, H. Farid, Y. Gu, M. He, K. Nagano, and H. Li, "Protecting world leaders against deep fakes." in *CVPR workshops*, vol. 1, no. 38, 2019.
- [13] S. Fernandes, S. Raj, E. Ortiz, I. Vintila, M. Salter, G. Urosevic, and S. Jha, "Predicting heart rate variations of deepfake videos using neural ode," in *Proceedings of the IEEE/CVF international conference on computer vision workshops*, 2019, pp. 0–0.
- [14] R. Wang, F. Juefei-Xu, M. Luo, Y. Liu, and L. Wang, "Faketagger: Robust safeguards against deepfake dissemination via provenance tracking," in *Proceedings of the 29th ACM international conference on multimedia*, 2021, pp. 3546–3555.

- [15] T. Wang, M. Huang, H. Cheng, B. Ma, and Y. Wang, "Robust identity perceptual watermark against deepfake face swapping," *arXiv preprint arXiv:2311.01357*, 2023.
- [16] T. Wang, M. Huang, H. Cheng, X. Zhang, and Z. Shen, "Lampmark: Proactive deepfake detection via training-free landmark perceptual watermarks," in *Proceedings of the 32nd ACM International Conference on Multimedia*, 2024, pp. 10515–10524.
- [17] Y. Yang, C. Liang, H. He, X. Cao, and N. Z. Gong, "Faceguard: Proactive deepfake detection," *arXiv preprint arXiv:2109.05673*, 2021.
- [18] N. Beuve, W. Hamidouche, and O. Déforges, "Waterlo: Protect images from deepfakes using localized semi-fragile watermark," in *Proceedings of the IEEE/CVF international conference on computer vision*, 2023, pp. 393–402.
- [19] P. Neekhara, S. Hussain, X. Zhang, K. Huang, J. McAuley, and F. Koushanfar, "Facesigns: Semi-fragile watermarks for media authentication," *ACM Transactions on Multimedia Computing, Communications and Applications*, vol. 20, no. 11, pp. 1–21, 2024.
- [20] A. Wachi, "Failure-scenario maker for rule-based agent using multi-agent adversarial reinforcement learning and its application to autonomous driving," *Twenty-Eighth International Joint Conference on Artificial Intelligence*, 2019.
- [21] J. Foerster, G. Farquhar, T. Afouras, N. Nardelli, and S. Whiteson, "Counterfactual multi-agent policy gradients," in *Proceedings of the AAAI conference on artificial intelligence*, vol. 32, no. 1, 2018.
- [22] J. Wang, W. Xu, Y. Gu, W. Song, and T. C. Green, "Multi-agent reinforcement learning for active voltage control on power distribution networks," *Advances in neural information processing systems*, vol. 34, pp. 3271–3284, 2021.
- [23] Z. Peng, Q. Li, K. M. Hui, C. Liu, and B. Zhou, "Learning to simulate self-driven particles system with coordinated policy optimization," *Advances in neural information processing systems*, vol. 34, pp. 10784–10797, 2021.
- [24] M. Kouzehgar, M. Meghjani, and R. Bouffanais, "Multi-agent reinforcement learning for dynamic ocean monitoring by a swarm of buoys," in *Global Oceans 2020: Singapore-US Gulf Coast*. IEEE, 2020, pp. 1–8.
- [25] J. Wang, Z. Ren, B. Han, J. Ye, and C. Zhang, "Towards understanding cooperative multi-agent q-learning with value factorization," *Advances in Neural Information Processing Systems*, vol. 34, pp. 29142–29155, 2021.
- [26] S. Li, Y. Wu, X. Cui, H. Dong, F. Fang, and S. Russell, "Robust multi-agent reinforcement learning via minimax deep deterministic policy gradient," in *Proceedings of the AAAI conference on artificial intelligence*, vol. 33, no. 01, 2019, pp. 4213–4220.
- [27] T. van der Heiden, C. Salge, E. Gavves, and H. van Hoof, "Robust multi-agent reinforcement learning with social empowerment for coordination and communication," *arXiv preprint arXiv:2012.08255*, 2020.
- [28] A. Bukharin, Y. Li, Y. Yu, Q. Zhang, Z. Chen, S. Zuo, C. Zhang, S. Zhang, and T. Zhao, "Robust multi-agent reinforcement learning via adversarial regularization: Theoretical foundation and stable algorithms," *Advances in neural information processing systems*, vol. 36, pp. 68121–68133, 2023.
- [29] L. Yuan, F. Chen, Z. Zhang, and Y. Yu, "Communication-robust multi-agent learning by adaptable auxiliary multi-agent adversary generation," *Frontiers of Computer Science*, vol. 18, no. 6, p. 186331, 2024.
- [30] A. Radford, J. W. Kim, C. Hallacy, A. Ramesh, G. Goh, S. Agarwal, G. Sastry, A. Askell, P. Mishkin, J. Clark, *et al.*, "Learning transferable visual models from natural language supervision," in *International conference on machine learning*. PmlR, 2021, pp. 8748–8763.
- [31] D. P. Kingma and J. Ba, "Adam: A method for stochastic optimization," *arXiv preprint arXiv:1412.6980*, 2014.
- [32] T. Karras, S. Laine, and T. Aila, "A style-based generator architecture for generative adversarial networks," in *Proceedings of the IEEE/CVF conference on computer vision and pattern recognition*, 2019, pp. 4401–4410.
- [33] Z. Liu, P. Luo, X. Wang, and X. Tang, "Deep learning face attributes in the wild," in *Proceedings of the IEEE international conference on computer vision*, 2015, pp. 3730–3738.
- [34] T. Karras, T. Aila, S. Laine, and J. Lehtinen, "Progressive growing of gans for improved quality, stability, and variation," *arXiv preprint arXiv:1710.10196*, 2017.
- [35] Y. He, N. Yu, M. Keuper, and M. Fritz, "Beyond the spectrum: Detecting deepfakes via re-synthesis," *arXiv preprint arXiv:2105.14376*, 2021.
- [36] S.-Y. Wang, O. Wang, R. Zhang, A. Owens, and A. A. Efros, "Cnn-generated images are surprisingly easy to spot... for now," in *Proceedings of the IEEE/CVF conference on computer vision and pattern recognition*, 2020, pp. 8695–8704.
- [37] N. Bonettini, E. D. Cannas, S. Mandelli, L. Bondi, P. Bestagini, and S. Tubaro, "Video face manipulation detection through ensemble of cnns," in *2020 25th international conference on pattern recognition (ICPR)*. IEEE, 2021, pp. 5012–5019.
- [38] L. Chai, D. Bau, S.-N. Lim, and P. Isola, "What makes fake images detectable? understanding properties that generalize," in *European conference on computer vision*. Springer, 2020, pp. 103–120.
- [39] C. Wang and W. Deng, "Representative forgery mining for fake face detection," in *Proceedings of the IEEE/CVF conference on computer vision and pattern recognition*, 2021, pp. 14923–14932.
- [40] K. Shiohara and T. Yamasaki, "Detecting deepfakes with self-blended images," in *Proceedings of the IEEE/CVF conference on computer vision and pattern recognition*, 2022, pp. 18720–18729.
- [41] T. Fernando, C. Fookes, S. Sridharan, and S. Denman, "Cross-branch orthogonality for improved generalization in face deepfake detection," *arXiv preprint arXiv:2505.04888*, 2025.
- [42] X. Zhao, K. Zhang, Z. Su, S. Vasani, I. Grishchenko, C. Kruegel, G. Vigna, Y.-X. Wang, and L. Li, "Invisible image watermarks are provably removable using generative ai," in *Advances in Neural Information Processing Systems*, 2024.
- [43] N. Lukas, A. Diaa, L. Fenaux, and F. Kerschbaum, "Leveraging optimization for adaptive attacks on image watermarks," *The Twelfth International Conference on Learning Representations (ICLR 2024)*, 2024.
- [44] R. Chen, X. Chen, B. Ni, and Y. Ge, "Simswap: An efficient framework for high fidelity face swapping," in *MM '20: The 28th ACM International Conference on Multimedia*, 2020.
- [45] C. Xu, J. Zhang, Y. Han, G. Tian, X. Zeng, Y. Tai, Y. Wang, C. Wang, and Y. Liu, "Designing one unified framework for high-fidelity face reenactment and swapping," in *European conference on computer vision*. Springer, 2022, pp. 54–71.
- [46] F. Rosberg, E. E. Aksoy, F. Alonso-Fernandez, and C. Englund, "Facedancer: Pose-and occlusion-aware high fidelity face swapping," in *Proceedings of the IEEE/CVF winter conference on applications of computer vision*, 2023, pp. 3454–3463.
- [47] S. Bounareli, C. Tzelepis, V. Argyriou, I. Patras, and G. Tzimirooulos, "Hyperreenact: one-shot reenactment via jointly learning to refine and retarget faces," in *Proceedings of the IEEE/CVF international conference on computer vision*, 2023, pp. 7149–7159.



**Tharindu Fernando** received his BSc (special degree in computer science) from the University of Peradeniya, Sri Lanka, and his PhD from Queensland University of Technology (QUT), Australia. He is currently a Postdoctoral Research Fellow in the Signal Processing, Artificial Intelligence, and Vision Technologies (SAIVT) research program at the School of Electrical Engineering and Robotics at Queensland University of Technology (QUT). He is a recipient of the 2019 QUT University Award for Outstanding Doctoral Thesis, the QUT Early Career Researcher Award in 2022, the QUT Faculty of Engineering Early Career Achievement Award in 2024, and the 2024 National Intelligence Post-Doctoral Grant. His research interests include Artificial Intelligence, Computer Vision, Deep Learning, Bio Signal Processing, and Video Analytics.



**Clinton Fookes** (Senior Member, IEEE) received the B.Eng. in Aerospace/Avionics, the MBA degree, and the Ph.D. degree in computer vision. He is currently the Associate Dean Research, a Professor of Vision and Signal Processing, and Co-Director of the SAIVT Lab (Signal Processing, Artificial Intelligence and Vision Technologies) with the Faculty of Engineering at the Queensland University of Technology, Brisbane, Australia. His research interests include computer vision, machine learning, signal processing, and artificial intelligence. He serves on

the editorial boards for IEEE TRANSACTIONS ON IMAGE PROCESSING and Pattern Recognition. He has previously served on the Editorial Board for IEEE TRANSACTIONS ON INFORMATION FORENSICS AND SECURITY. He is a Fellow of the International Association of Pattern Recognition, a Fellow of the Australian Academy of Technological Sciences and Engineering, and a Fellow of the Asia-Pacific Artificial Intelligence Association. He is a Senior Member of the IEEE and a multi-award winning researcher including an Australian Institute of Policy and Science Young Tall Poppy, an Australian Museum Eureka Prize winner, Engineers Australia Engineering Excellence Award, Australian Defence Scientist of the Year, and a Senior Fulbright Scholar.



**Sridha Sridharan** has obtained an MSc (Communication Engineering) degree from the University of Manchester, UK, and a PhD degree from the University of New South Wales, Australia. He is currently with the Queensland University of Technology (QUT) where he is a Professor in the School of Electrical Engineering and Robotics. He has published over 600 papers consisting of publications in journals and in refereed international conferences in the areas of Image and Speech technologies during the period 1990-2023. During this period he has also

graduated 85 PhD students in the areas of Image and Speech technologies. Prof Sridharan has also received a number of research grants from various funding bodies including the Commonwealth competitive funding schemes such as the Australian Research Council (ARC) and the National Security Science and Technology (NSST) unit. Several of his research outcomes have been commercialised.